

A UNIFIED MOBILITY MODEL FOR DEVICE SIMULATION—II. TEMPERATURE DEPENDENCE OF CARRIER MOBILITY AND LIFETIME

D. B. M. KLAASSEN

Philips Research Laboratories, P.O. Box 80000, 5600 JA Eindhoven, The Netherlands

(Received 14 August 1991; in revised form 18 December 1991)

Abstract—In Part I we presented the first physics-based analytical model that unifies the descriptions of majority and minority carrier mobility and that includes screening of the impurities by charge carriers, electron-hole scattering and clustering of impurities. Here the model is extended to include the full temperature dependence of both majority and minority carrier mobility. Based on our model and experimental data on the minority carrier diffusion length as a function of temperature, the temperature dependence of the carrier lifetime is determined. The model is especially suited for device simulation purposes, because the carrier mobility is given as an analytical function of the donor, acceptor, electron and hole concentrations and of the temperature.

1. INTRODUCTION

In a previous paper[1] (hereafter referred to as Part I) we published a mobility model that unifies the description of majority and minority carrier mobility. Using this analytical model, experimental data on majority and minority carrier mobility and mobility data on electron-hole scattering are accurately described. In this paper we describe the incorporation of the temperature dependence of the carrier mobility in our model and make a comparison with experimental data. The main features of the model and a limited comparison with experimental data have been published elsewhere[2].

Comparing experimental mobility data as a function of temperature with model calculations is hampered by the incomplete ionization of the doping ions. Moreover, only data on the minority carrier diffusion length as a function of temperature are available[3-5]. Consequently, the temperature dependence of the lifetime is needed in order to calculate the temperature dependence of diffusion length from our mobility model. Both problems are dealt with, leading to a consistent model description of the experimental data on the diffusion length as a function of temperature.

2. TEMPERATURE DEPENDENCE OF THE MOBILITY

In this section the temperature dependence of the four contributions to the mobility, as presented in Part I, is discussed.

2.1. Lattice scattering

For the lattice scattering mobility, $\mu_{i,L}$ [see eqn (2) of Part I], we use the well-known power dependence on temperature (see e.g. Refs [6,7]):

$$\mu_{i,L} = \mu_{\max} \left(\frac{300}{T} \right)^{\theta_i}, \quad (1)$$

where the subscript i stands for e or h. The parameters θ_i will be determined in comparison with experimental data.

2.2. Majority impurity scattering

For the majority impurity scattering mobility, $\mu_{i,I}$ given by eqn (5) of Part I, we use the temperature dependence as implied by the Conwell-Weisskopf and Brooks-Herring approaches. From eqn (A5) in the Appendix of Part I we see that we can then still use eqn (5) of Part I, but:

with

$$\mu_{i,N} = \frac{\mu_{\max}^2}{\mu_{\max} - \mu_{\min}} \left(\frac{T}{300} \right)^{3\alpha_1 - 1.5} \quad (2a)$$

and

$$\mu_{i,c} = \frac{\mu_{\min} \mu_{\max}}{\mu_{\max} - \mu_{\min}} \left(\frac{300}{T} \right)^{0.5}, \quad (2b)$$

where the subscripts (i, I) stand for (e, D) or (h, A). As the parameter α_1 stems from the description of the majority carrier mobility as a function of impurity concentration [see eqn (1) of Part I], no additional parameters are introduced.

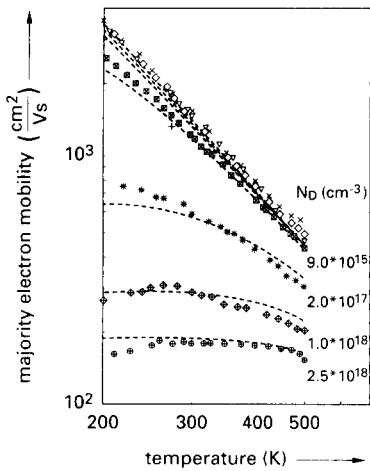


Fig. 1. Majority electron mobility as a function of temperature for various donor concentrations. Dashed lines represent model calculations and symbols represent the experimental data of Li and Thurber[8,9]: \times , $1.2 \times 10^{14} \text{ cm}^{-3}$; \diamond , $4.0 \times 10^{14} \text{ cm}^{-3}$; \triangle , $1.0 \times 10^{15} \text{ cm}^{-3}$; \boxtimes , $9.0 \times 10^{15} \text{ cm}^{-3}$; $*$, $2.0 \times 10^{17} \text{ cm}^{-3}$; \oplus , $1.0 \times 10^{18} \text{ cm}^{-3}$; and \oplus , $2.5 \times 10^{18} \text{ cm}^{-3}$.

At this point we have specified the temperature dependence of the two contributions which determine the majority carrier mobility. Consequently, the majority carrier mobility can be calculated as a function of temperature and compared to the experimental data in order to determine the parameters θ_e (see Figs 1 and 2). The values obtained are $\theta_e = 2.285$ and $\theta_h = 2.247$. From Figs 1 and 2 it can be seen that with the introduction of only two parameters a good description of the majority carrier mobility as a function of temperature is obtained for temperatures higher than 200 K.

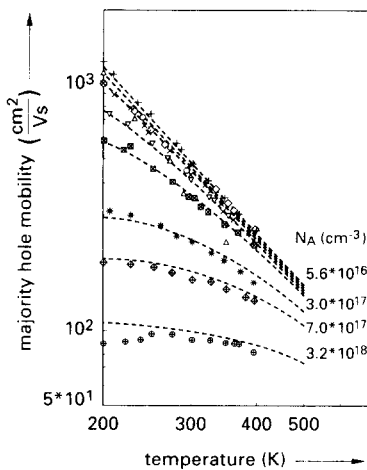


Fig. 2. Majority hole mobility as a function of temperature for various acceptor concentrations. Dashed lines represent model calculations and symbols represent the experimental data of Li[10,11]: $+$, $4.5 \times 10^{14} \text{ cm}^{-3}$; \times , $1.1 \times 10^{15} \text{ cm}^{-3}$; \diamond , $4.5 \times 10^{15} \text{ cm}^{-3}$; \triangle , $2.1 \times 10^{16} \text{ cm}^{-3}$; \boxtimes , $5.6 \times 10^{16} \text{ cm}^{-3}$; $*$, $3.0 \times 10^{17} \text{ cm}^{-3}$; \oplus , $7.0 \times 10^{17} \text{ cm}^{-3}$; and \oplus , $3.2 \times 10^{18} \text{ cm}^{-3}$.

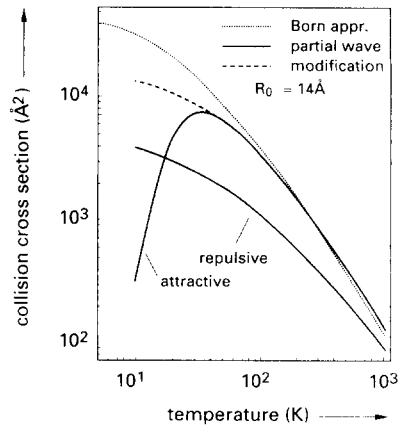


Fig. 3. Collision cross-sections for momentum relaxation calculated as function of the temperature for a screening radius of 14 \AA (as in Fig. 6 of Ref. [12]). The dotted line represents the Born (or Brooks-Herring) approximation; the solid lines represent the partial wave method; and the dashed line represents the modification suggested.

2.3. Minority impurity scattering

The minority impurity scattering mobility is given by eqn (10) of Part I. In these expressions $\mu_{e,D}$ and $\mu_{h,A}$ have the temperature dependence described in the previous subsection. The parameters P_e and P_h depend quadratically on temperature [see eqns (16), (8) and (A3) of Part I]. Furthermore, for fixed P the function G depends on temperature [see eqn (9) and Fig. 2 of Part I]. For values of P larger than unity the combined effect of the temperature dependences of the parameter P and function G yields for $G(P)$ a value that decreases with temperature. As can be seen from Fig. 2 of Part I, however, $G(P)$ reaches a minimum at values of P between 0.1 and 1, which might result in a different dependence of $G(P)$ on temperature. This minimum in the function G originates from the fact that the collision cross-section for an attractive potential reaches a maximum as a function of the temperature (see Fig. 3). This maximum is related to the Ramsauer effect (see Ref. [12]). Although in practice the Ramsauer effect may occur

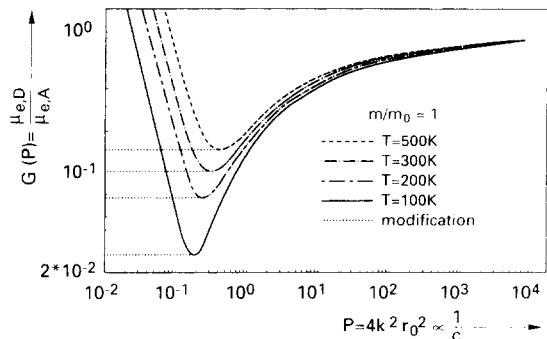


Fig. 4. The function $G(P)$ calculated as a function of P for four different temperatures and an effective carrier mass equal to the free carrier mass (see Fig. 2 of Part I). The dotted line represents the modification suggested (see text).

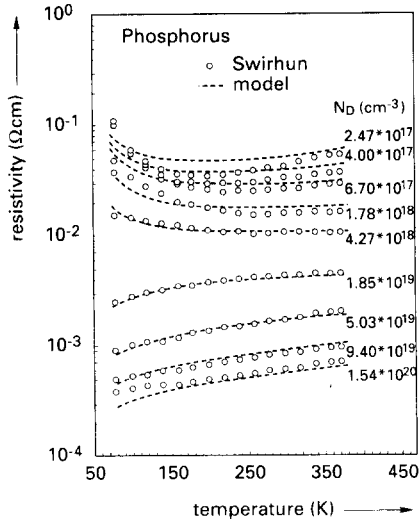


Fig. 5. Resistivity of P-doped Si as a function of temperature for various impurity concentrations. The symbols indicate the experimental data of Swirhun[3] and the dashed lines indicate our model calculations.

in Si, the Conwell–Weisskopf and Brooks–Herring (or Born) approximations, which form the basis for the temperature dependence of $\mu_{e,D}$ and $\mu_{h,A}$ in eqn (10) of Part I, do not incorporate such interference effects (see Fig. 3). Consequently these interference effects should also be removed from the function G in order to obtain the correct values for $\mu_{e,A}$ and $\mu_{h,D}$, respectively. This can be done effectively by taking $G(P)$ for values of P smaller than the value at which the minimum is reached, equal to the value at that minimum (see Fig. 4). In this way, a temperature dependence for the collision cross-section for an attractive potential indicated by the dashed line in Fig. 3 is obtained.

2.4. Electron–hole scattering

The electron–hole scattering mobility is given by eqn (13) of Part I. Again, the temperature dependence of $\mu_{e,D}$ and $\mu_{h,A}$ is involved and, as indicated in the previous subsection, the parameters P_e and P_h depend quadratically on temperature. The function F , however, is independent of temperature [see eqn (12) and Fig. 3 of Part I]. Consequently, this yields for $F(P)$ a value that increases with decreasing temperature. So the electron–hole scattering mobility as well as the minority impurity scattering mobility increase with respect to the majority impurity scattering mobility with decreasing temperature. Consequently, at high concentrations where the lattice scattering is negligible, the ratio between minority carrier mobility and the majority carrier mobility increases with decreasing temperature.

3. EFFECTS OF INCOMPLETE IONIZATION

At low temperatures the impurity atoms are only partly ionized. In the temperature range shown in

Figs 1 and 2 the ionization is almost complete. However, the data on the minority carrier diffusion length as a function temperature range down to 100 K for electrons[3,4], and even down to 30 K for holes[5]. At these low temperatures only a small fraction of the impurity atoms will be ionized. In this section we will investigate the effects of incomplete ionization on the minority carrier mobility as a function of temperature.

The fraction of ionized impurity atoms can be calculated using a quite simple method (see e.g. Ref. [13]). A problem of this method is that at a concentration of about $3 \times 10^{18} \text{ cm}^{-3}$ the ionization energy goes to zero. At that concentration the ionization is still incomplete, while the method cannot be used for higher concentrations. Kuzmicz published an analytical approximation for the ionized fraction as a function of temperature[14]. His results are based on a more sophisticated method and show complete ionization at high concentrations. Consequently, they can be used over the whole concentration range, but only for temperatures higher than 250 K. Therefore, we used the former method, modified in the activation energy model the power dependence on the concentration and allowed for negative activation energies. The parameters in the activation energy model were determined in a fit to experimental resistivity data as a function of temperature and impurity concentration. In this fit the majority carrier mobility was calculated as in Figs 1 and 2 (see Section 2.2), while the ionized impurity concentration in the mobility formulation and the carrier concentration were obtained from the ionized fraction. The comparison of model calculations and experimental data in Fig. 5 shows that at high concentrations the agreement is good, while at low concentrations the deviations are smaller than 30%. The resulting ionized fraction is shown in Fig. 6 as a function of temperature and impurity concentration. From this figure it can be seen that, like Kuzmicz[14], we obtained complete ionization at concentrations larger than 10^{19} cm^{-3} .

Using the ionized fraction as a function of temperature and concentration, we can now investigate the influence of the incomplete ionization on the

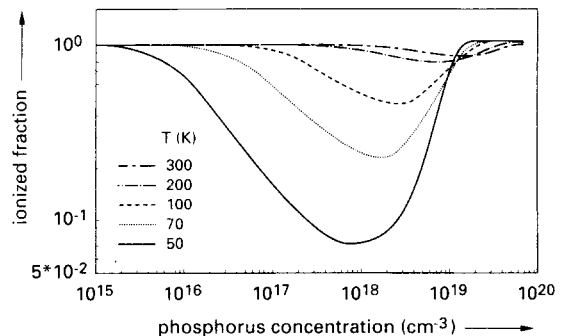


Fig. 6. Ionized fraction as a function of concentration for various temperatures.

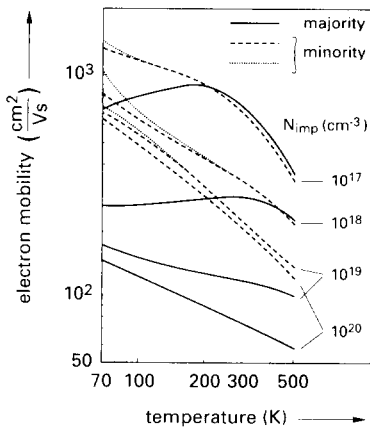


Fig. 7. Electron mobility as a function of temperature for various impurity concentrations. Dashed lines indicate model calculations for the minority electron mobility using complete ionization; dotted lines indicate model calculations for the minority electron mobility using a temperature-dependent ionization (see Fig. 6); and solid lines indicate the majority electron mobility.

minority carrier mobility as a function of temperature. It should be noted that once the temperature dependence of the lattice scattering mobility and majority impurity scattering mobility is known, the temperature dependence of the minority carrier mobility itself is completely fixed by functions $G(P)$ and $F(P)$ and parameters determined in Part I. In Figs 7 and 8 the temperature dependence of the minority carrier mobility is shown with complete and incomplete ionization. As can be seen from these figures, incomplete ionization has only a very small effect on the minority carrier mobility. Furthermore, the minority carrier mobility shows a temperature behaviour distinctly different from the majority carrier mobility. Moreover, it shows that at all temperatures the

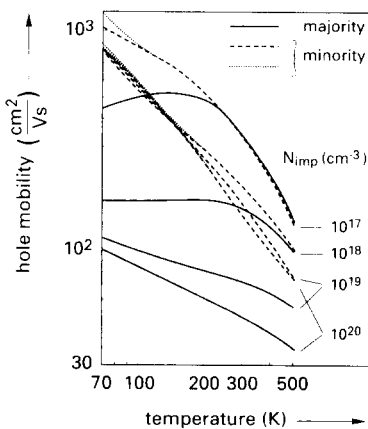


Fig. 8. Hole mobility as a function of temperature for various impurity concentrations. Dashed lines indicate model calculations for the minority hole mobility using complete ionization; dotted lines indicate model calculations for the minority hole mobility using a temperature-dependent ionization; and solid lines indicate the majority hole mobility.

minority carrier mobility decreases (or stays constant) with increasing impurity concentration. This is in disagreement with the results reported by Swirhun *et al.*[4] and Wang *et al.*[5]. The origin of this discrepancy will be discussed in the following sections.

4. TEMPERATURE DEPENDENCE OF CARRIER LIFETIME

As mentioned in the introduction, only data on the minority carrier diffusion length as a function of temperature are available[3-5]. Consequently, besides the concentration dependence, the temperature dependence of the lifetime is also needed in order to compare our model with these data.

The concentration dependence of the lifetime for electrons τ_e and for holes τ_h can be described (see e.g. Ref. [13]):

by

$$\tau_e^{-1} = \tau_{0,e}^{-1} + C_{SRH,e} N_t + C_{Aug,e} p^2, \tag{3a}$$

and

$$\tau_h^{-1} = \tau_{0,h}^{-1} + C_{SRH,h} N_t + C_{Aug,h} n^2, \tag{3b}$$

where $\tau_{0,i}$ is the intrinsic lifetime, $C_{SRH,i}$ is the Shockley-Read-Hall coefficient, N_t is the total impurity concentration, $C_{Aug,i}$ is the Auger coefficient, and p and n are the hole and electron concentrations. Mid-gap centres are most effective in the steady-state Shockley-Read-Hall process. Recombination involving these centres leads according to theory[15-17] and various experiments[18-21] to lifetimes increasing with temperature. For the Auger-limited lifetime, however, theory[22] and experiments[23,24] show a decrease with increasing temperatures. Consequently, the terms in eqn (3) representing the Shockley-Read-Hall and Auger process, respectively, should have separate temperature dependences:

$$\tau_e^{-1} = (\tau_{0,e}^{-1} + C_{SRH,e} N_t) \left(\frac{300}{T}\right)^\gamma + (C_{Aug,e} p^2) \left(\frac{T}{300}\right)^\delta, \tag{4}$$

where T is the temperature, and γ and δ are expected to be positive. A similar expression should hold for the hole minority lifetime. It should be noted that in the comparison of experimental data and model calculations $\tau_{0,e}$ plays a minor role (see below and Table 1).

Table 1. Model parameters for the minority carrier lifetime [see eqn (4)]

Parameter	Electrons	Holes
τ_0 (ms)	2.50	2.50
C_{SRH} ($10^{13} \text{ cm}^3 \text{ s}^{-1}$)	3.00	11.76
C_{Aug} ($10^{31} \text{ cm}^6 \text{ s}^{-1}$)	1.83	2.78
γ	1.77	0.57
δ	1.18	0.72

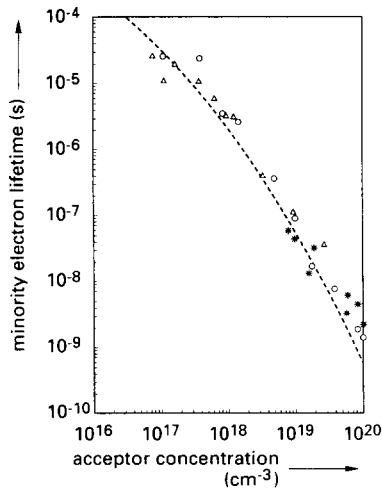


Fig. 9. Minority electron lifetime as a function of acceptor concentration at 300 K. Symbols represent experimental data from the literature: \circ [23]; \triangle [25]; $*$ [26]. The dashed curve represents eqn (3a) with the parameters given in Table 1.

To determine accurately the parameters $C_{SRH,i}$, $C_{Aug,i}$, γ and δ , one would need a set of lifetime data as a function of concentration and temperature. Such data is however very scarce in literature. Dziejwior and Schmid performed their measurements only at three temperatures[23]. At this point it is interesting to note which models were used by the authors who performed the experiments. Swirhun *et al.*[4] took the minority carrier lifetime to be independent of temperature and arrived at a temperature dependence of the minority electron mobility in disagreement with our model (see Section 3). Earlier, Swirhun[3] used a power dependence on temperature for the lifetime ($\tau_c \propto T^x$) to interpret the same diffusion length data. The power x was varied between 1 at low concen-

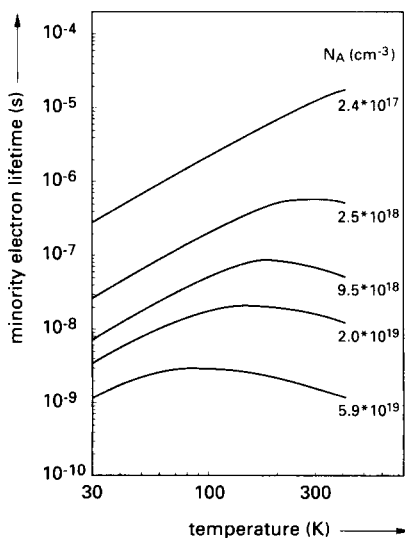


Fig. 10. Minority electron lifetime calculated as a function of temperature for various acceptor concentrations [see eqn (4) and Table 1].

trations and about -0.4 at high concentrations. This is in agreement with a Shockley–Read–Hall limited lifetime at low concentrations and an Auger limited lifetime at high concentrations. From eqn (4), however, it will be clear that a single power dependence will not suffice to describe the lifetime over a large temperature range for these two competing processes (see also Fig. 10). Wang *et al.*[5] used a lifetime increasing linearly with decreasing temperatures down to 30 K. They found a temperature dependence of the minority hole mobility that is in disagreement with our model (see Section 3 and Fig. 8). This is not surprising, because at low temperatures the lifetime is determined by the Shockley–Read–Hall process and decreases with decreasing temperature (see also Fig. 10).

As mentioned in the previous section, the temperature behaviour and concentration dependence of the minority carrier mobility are completely correlated in our model. Therefore, we calculated the minority carrier diffusion length using our mobility model and the lifetime model given by eqn (4). The parameters in the latter model were determined from a simultaneous fit of:

- the diffusion length to the experimental data as a function of temperature and concentration[3–5]; and
- the minority carrier lifetime to the experimental data as a function of concentration (see Fig. 9).

The results for the diffusion length will be presented in the next section, while here the lifetime will be discussed. The parameters found for the lifetime model are given in Table 1. Using these parameters the minority carrier lifetimes are well described as a function of concentration, as can be seen from Fig. 9 for electrons. The temperature dependence of the Shockley–Read–Hall lifetime is different for minority electrons and holes, which has also been observed in direct experiments on deep levels[18,20,21]. In Table 2 the values found for the Auger coefficients are compared with experimental and theoretical data. For both types of carriers the trends as a function of temperature are in good agreement, while for holes almost identical values were found.

In Fig. 10, finally, for minority electrons the lifetime as a function of temperature is shown for the

Table 2. Comparison of Auger coefficients (in $10^{-31} \text{ cm}^6 \text{ s}^{-1}$) from this work and from literature for various temperatures T . It should be noted that the values listed as “this work” have been calculated from $C_{Aug}(T/300)^6$ in order to facilitate comparison

T (K)	Reference	Electrons	Holes
77	This work	0.37	1.0
	Experimental [23]	0.78	2.3
	Theoretical [22]		1.8–2.4
300	This work	1.8	2.8
	Experimental [23]	0.99	2.8
	Theoretical [22]		2.7
400	This work	2.6	3.4
	Experimental [23]	1.2	2.8
	Theoretical [22]		2.8

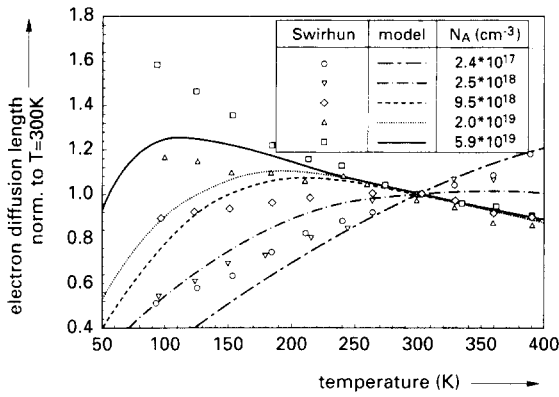


Fig. 11. Minority electron diffusion length as a function of temperature for various acceptor concentrations and normalized to its value at 300 K. Symbols indicate the experimental data of Swirhun[3]; curves indicate the model calculations.

acceptor concentrations used by Swirhun in the experiments on the diffusion lengths[3] (see Section 5). From this figure two recombination mechanisms can clearly be distinguished: the Shockley-Read-Hall process at low temperatures and concentrations vs the Auger process at high temperatures and concentrations.

5. COMPARISON WITH EXPERIMENTAL DIFFUSION LENGTH DATA

From the previous section it will be clear that for a comparison between the minority carrier mobility from our model and experiments, we have to use the diffusion length data. In order to separate the temperature dependence from the concentration dependence, we normalized the data[3,5] to values at 300 K (see Figs 11 and 12). Moreover, for the data of Swirhun this procedure was necessary because for low concentrations the diffusion lengths were stated to be too small due to a systematic error. The

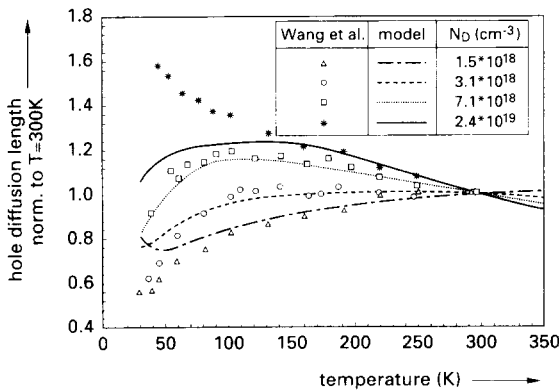


Fig. 12. Minority hole diffusion length as a function of temperature for various donor concentrations and normalized to its value at 300 K. Symbols indicate the experimental data of Wang *et al.*[5]; curves indicate the model calculations.

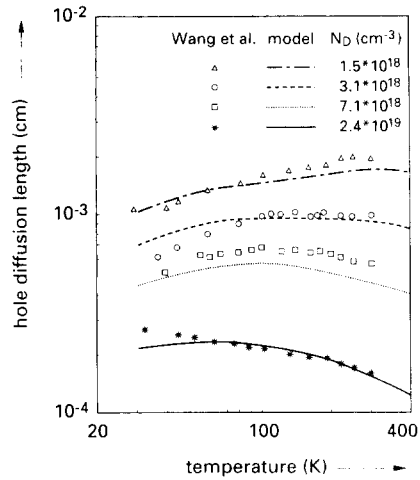


Fig. 13. Minority hole diffusion length as a function of temperature for various donor concentrations. Symbols indicate the experimental data of Wang *et al.*[5]; curves indicate the model calculations.

temperature dependence, however, was unaffected[3]. In Figs 11 and 12 the results of the interpretation mentioned in the previous section are compared with the experimental data. For the normalized minority electron diffusion length, differences between experimental data and model are smaller than 10% for temperatures higher than 150 K. For the normalized minority hole diffusion length, good agreement between experimental data and model calculations is obtained for temperatures even down to 100 K. The minority hole diffusion lengths measured by Wang *et al.*[5] can also be compared with our model calculations without normalization. To this end, we reduced the coefficient $C_{SRH,h}$, which in contrast to $C_{Aug,h}$ may be dependent on wafer processing, with 30% in order to obtain perfect agreement between our lifetime model and the lifetime data of Wang at 300 K. The minority hole diffusion lengths obtained are shown in Fig. 13. From this figure it can be seen that over the whole temperature region and for all donor concentrations the difference between model and experimental data is less than 20%.

6. CONCLUSIONS

The unified mobility model published earlier (see Section 1) has been extended to describe the temperature dependence of both majority and minority carrier mobility. Apart from the parameters θ_i in the lattice scattering mobility, no additional parameters were introduced to obtain the temperature dependence of the minority carrier mobility. Incomplete ionization was shown to play a minor role in the minority carrier mobility as a function of temperature. The temperature dependence of the minority carrier lifetime, however, is of crucial importance in the interpretation of diffusion length data as a function of temperature. Using a realistic model for the

minority carrier lifetime we obtained good agreement between our model and experimental data on the diffusion length as a function of temperature. Most remarkable is that our model does not predict a minority carrier mobility sharply increasing with concentration at low temperatures. This is in contrast to earlier interpretations of the same data[4,5], in which too simple models for the carrier lifetime were used.

In conclusion, it may be stated that the first physics-based analytical model has been presented (here and in Part I), that unifies the descriptions of majority and minority carrier mobility and that includes the full temperature dependence of both majority and minority carrier mobility. Using this model good agreement with all available experimental data has been obtained. Because the carrier mobility is given as an analytical function of the donor, acceptor, electron and hole concentrations and of the temperature, the model is especially suited for device simulation purposes.

Acknowledgement—Part of this work was funded by ESPRIT Project 2016.

REFERENCES

1. D. B. M. Klaassen, *Solid-St. Electron.* **35**, 953 (1992).
2. D. B. M. Klaassen, *IEDM Tech. Dig.*, p. 357 (1990).
3. S. E. Swirhun, Ph.D. Dissertation, Stanford University, CA (1987).
4. S. E. Swirhun, D. E. Kane and R. M. Swanson, *IEDM Tech. Dig.*, p. 298 (1988).
5. C. H. Wang, K. Misiakos and A. Neugroschel, *Appl. Phys. Lett.* **57**, 159 (1990).
6. F. J. Morin and J. P. Maita, *Phys. Rev.* **96**, 28 (1954).
7. G. W. Ludwig and R. L. Watters, *Phys. Rev.* **101**, 1699 (1956).
8. S. S. Li and W. R. Thurber, *Solid-St. Electron.* **20**, 609 (1977).
9. S. S. Li, *National Bureau of Standards, Special Publication 400-33*. Washington, DC (1977).
10. S. S. Li, *Solid-St. Electron.* **21**, 1109 (1978).
11. S. S. Li, *National Bureau of Standards, Special Publication 400-47*. Washington, DC (1979).
12. F. J. Blatt, *J. Phys. Chem. Solids* **1**, 262 (1957).
13. H. C. de Graaff and F. M. Klaassen, *Compact Transistor Modelling for Circuit Design*. Springer, Wien (1990).
14. W. Kuzmicz, *Solid-St. Electron.* **29**, 1223 (1986).
15. M. Lax, *J. Phys. Chem. Solids* **8**, 66 (1959).
16. M. Lax, *Phys. Rev.* **119**, 1502 (1960).
17. S. R. Dhariwal and P. T. Landsberg, *J. Phys.: Condens. Matter* **1**, 569 (1989).
18. G. Bemski, *Phys. Rev.* **111**, 1515 (1958).
19. D. J. Sandiford, *J. Appl. Phys.* **30**, 1981 (1959).
20. A. F. Tasch and C. T. Sah, *Phys. Rev. B* **1**, 800 (1970).
21. W. Schmid and J. Reiner, *J. Appl. Phys.* **53**, 6250 (1982).
22. D. B. Laks, G. F. Neumark, A. Hangleiter and S. T. Pantelides, *Phys. Rev. Lett.* **61**, 1229 (1988).
23. J. Dziewior and W. Schmid, *Appl. Phys. Lett.* **31**, 346 (1977).
24. P. C. Mathur, R. P. Sharma, P. Saxena and J. D. Arora, *J. Appl. Phys.* **52**, 3651 (1981).
25. J. D. Beck and R. Conrardt, *Solid St. Commun.* **13**, 93 (1973).
26. S. E. Swirhun, Y.-H. Kwark and R. M. Swanson, *IEDM Tech. Dig.*, p. 24 (1986).